ACS OMEGA

Open Access

http://pubs.acs.org/journal/acsodf

Article

Modeling of the Carbohydrate Oxacarbenium Ionic Intermediates of Glycosylation Reactions with Explicit Account for Protective Group Effects

Alexey G. Gerbst,* Bozhena S. Komarova, Artem N. Vlasenko, and Nikolay E. Nifantiev*

Cite This: *ACS Omega* 2025, 10, 2305−2313

Read Online

ACCESS | Metrics & More | Article Recommendations | Supporting Information

ABSTRACT: O-Protected oxacarbenium ions are key intermediates of glycosylation reactions. The knowledge of their conformational preferences is crucial for choosing the correct blocking group pattern to achieve the required stereochemical outcome. This article describes a computational study of several glucosyl oxacarbenium cations. The primary aim was to address the challenge of modeling oxacarbenium structures with all explicit O-blocking groups present instead of their simplified models. There exists no physical method to directly measure the energy of such structures. Therefore, the DLPNO−CCSD(T) method was used as a reference, which is considered to give the most exact results, however, without the possibility of geometry optimizations. Three DFT methods were tried to compare their values to those computed with DLPNO−CCSD(T). Finally, the B3LYP-D3 combination is suggested as the best recommendation for future studies of complex carbohydrate reaction intermediates with explicit protective groups. Possible reasons for the relative stability of different conformers of glycosyl cations are discussed in terms of SCF and electron correlation energies. The results of the B3LYP-D3 method show a good correlation with several model glycosylation reactions.

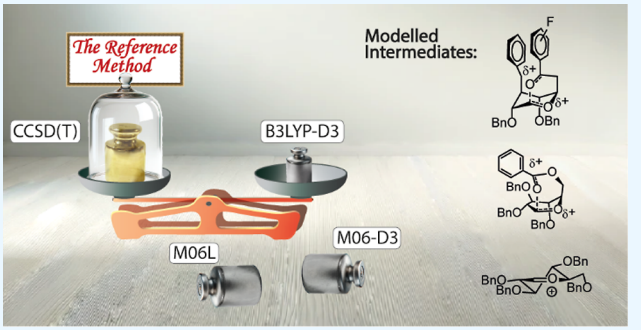

INTRODUCTION

The central question in glycosylation mechanism studies is the structure and conformation as well as electronic properties, reactivity, and stability of the intermediate glycosyl cation (Figure 1), along with the influence of the O- and N-blocking groups. This transient cyclic oxacarbenium ion formed from glycosyl donors during reactions plays a key role in determining stereochemistry, though not exclusively. Six-membered pyranose glycosyl cations exhibit considerable conformational mobility and diversity. They feature a planar, positively charged carbon atom stabilized by a lone pair of electrons on the intraring oxygen, serving as the pivotal reaction site (Figure 1). To explain how the glycosyl cation influences the stereochemistry of glycosylation, a two-conformer stereoelectronic model was developed.[1−3] According to this model, the glycosyl cation is represented by two adjacent minima on the potential energy surface. These two conformers are $^{4}\mathbf{H}_{3}$ and $^{3}\mathbf{H}_{4}$ (Figure 1), whose stability is explained by the optimal stabilization of the positive charge on the carbon atom by the lone pair on the intraring oxygen.

The side of the preferential nucleophilic attack on the planar carbon atom of the glycosyl cation is determined by whether $^{3}\mathbf{H}_{4}$ or $^{4}\mathbf{H}_{3}$ is more stable and by the geometry of the resultant transition state (Figure 1). A nucleophilic attack on the $^{3}\mathbf{H}_{4}$ conformation from the top side leads to a chairlike transition state (TS chair top $^{3}\mathbf{H}_{4}$), which possesses lower energy compared to the twist-boat conformation (TS twist bottom $^{3}\mathbf{H}_{4}$) that emerges from a nucleophilic attack from the bottom side. For the $^{4}\mathbf{H}_{3}$ conformation, the dynamics are inverted: a nucleophilic attack on the top face yields a twist-boat conformation (TS twist top $^{4}\mathbf{H}_{3}$) with higher energy, while an attack from the bottom face produces a more energetically favorable chairlike transition state (TS chair bottom $^{4}\mathbf{H}_{3}$).[1−4]

Thus, it appears important to correctly estimate relative energies of different conformations of glycosyl cations, particularly of $^{3}\mathbf{H}_{4}$ and $^{4}\mathbf{H}_{3}$. A variety of computational methods can be applied for this task: starting from molecular mechanics,[5,6] the RHF approach was also used.[7] An example of a combination of semiempirical, RHF, and DFT methods to the conformational analysis of tetrahydropyran oxacarbenium ions can be found in a work by Yang and Woerpel.[3] Nowadays, DFT is considered to be the most robust method for the conformational analysis of carbohydrates including, for example, glycosyl cations,[8−11] contact and solvent separated

Received: November 5, 2024
Revised: December 18, 2024
Accepted: December 23, 2024
Published: January 6, 2025

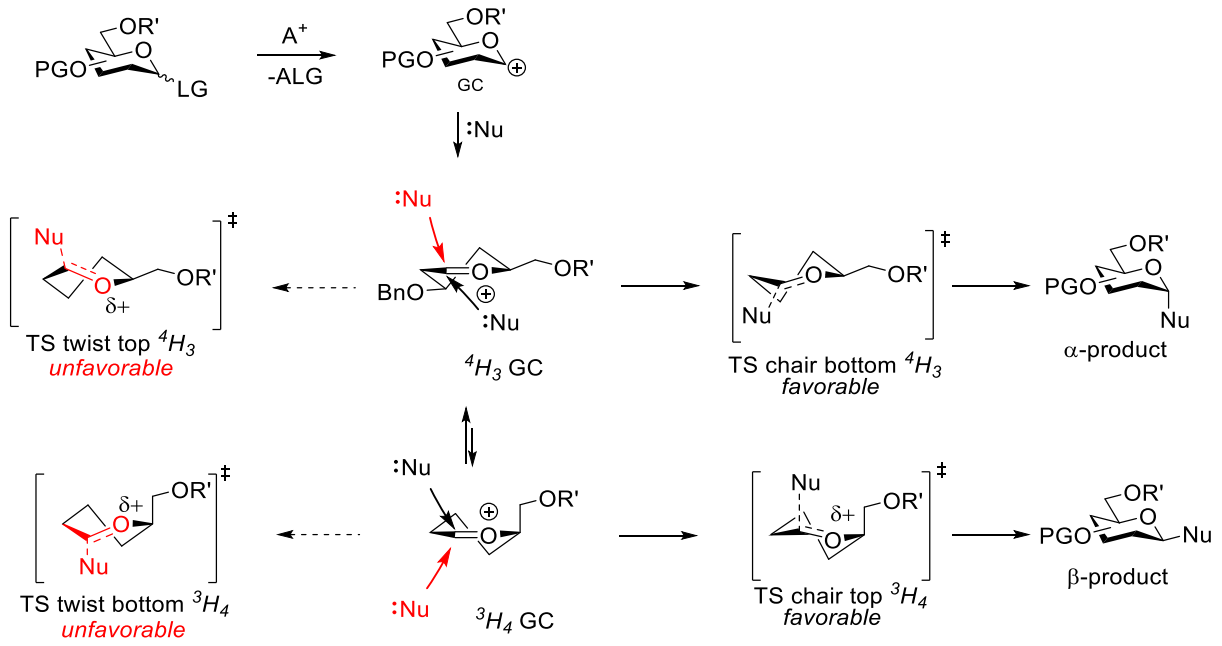

Figure 1. Plausible mechanism of the nucleophile (:Nu) attack on the glycosyl cation (GC) formed after the elimination of the leaving group (LG).

ion pairs,[12] transition states,[13] and stable carbohydrates of various nature.[14,15]

Higher level methods, such as MP2, are also employed,[16] and in the work by Marianski and coauthors,[17] a comparison of different DFT functionals with the DLPNO−CCSD(T) approach was carried out. However, the MP2 method still has high demands to the computational resources and when it comes to the modeling of carbohydrates, e.g., glycosyl cations, the DFT continues to be a method of choice. Apart from this, machine learning algorithms were employed for the prediction of glycosylation selectivity based on the DFT-optimized structures with explicit substituents.[18]

It should be noted that usually (except for ref 18) the DFT calculations are performed on the simplified model structures: particularly, protecting groups are removed or replaced with methoxy or acetoxy substituents even most recently.[19] Without 4,6-tethers such as benzylidene or formylidene or nearby or remote acyl groups affecting the ring puckering due to anchimeric assistance, the permethylated glucosyl and mannosyl cations have been reported to adopt conformations from both hemispheres: $^{4}\mathbf{C}_{1}$ (to which $^{4}\mathbf{H}_{3}$ belongs) and $^{1}\mathbf{C}_{4}$ (to which $^{3}\mathbf{H}_{4}$ belongs) (Figure 2). Most calculations are performed using CH_2Cl_2 as the solvent since it is the most commonly used solvent in glycosylations.

Satoh conducted a systematic study[20] of the influence of solvent polarity on the conformation of the oxocarbenium ion and its SSIP with OTf^- using computational methods. In this study, the conformations of the glucosyl oxocarbenium ion were optimized in the gas phase (as an approximation for toluene, diethyl ether, and dioxane) and in acetonitrile. In the $^{4}\mathbf{C}_{1}$ hemisphere, the glucosyl cation or its SSIP with the OTf ion is calculated to adopt conformations such as E_3 (with the relevant calculation methods indicated in Figure 2), $^{4}\mathbf{H}_{3}$, $^{4}\mathbf{E}$, and $^{2}\mathbf{H}_{3}-{}^{2}\mathbf{S}_{O}$. Between the two hemispheres, conformations $^{5}\mathbf{S}_{1}$ and $\mathbf{B}_{2,5}$ are found, with the latter being optimized in CH_3CN. The mannose cation (or its SSIP) is reported to adopt $^{4}\mathbf{H}_{3}$ and $\mathbf{E}_{3}$ in the $^{4}\mathbf{C}_{1}$ hemisphere or $^{O}\mathbf{S}_{2}-{}^{3}\mathbf{H}_{2}$ and $^{3}\mathbf{E}$ in the $^{1}\mathbf{C}_{4}$ hemisphere.

Beyond these cases, nothing else is known about the conformations of unrestricted glycosyl cations bearing standard protecting groups like nonparticipating benzyl groups at least at three positions. To address this gap, we decided to investigate derivatives of the 2,3,4-tri-*O*-benzylated glucosyl cation bearing various acyl groups, Bn, Bz, TFB, or PFB (Figure 3) at O-6 using different DFT methods. Previously, it was demonstrated that acyl groups at the O-6 position of glucose could have α-stereocontrolling effect.[23] In our recent investigation,[24] we successfully applied M06L functional with the def2-TZVP basis set to study the conformational equilibrium during the rotation around the C5−C6 bond in glucosyl oxacarbenium cations bearing different substituents at the O6 atom (Figure 3). However, in the course of further development of this work, when we decided to compare relative energies of two different ring conformations of these cations, namely, $^{4}\mathbf{H}_{3}$ and $^{3}\mathbf{H}_{4}$, it appeared that for the per-*O*-benzylated glucosyl cation **1**, the M06L/def2-TZVP approximation predicts the latter to be a little more preferable. However, in the work by Yang and Woerpel,[3] the opposite tendency was observed. It seems clear that in our case, when a phenyl ring containing protecting groups is involved, the correct account for dispersion interactions plays a crucial role (Figure 4).

The state-of-the-art method of electronic energy calculations, DLPNO−CCSD(T), was employed for a deeper investigation of this problem. It was found that, contrary to the M06L/def2-TZVP approximation, the DLPNO−CCSD(T)/CC-PVTZ method considers $^{4}\mathbf{H}_{3}$ more preferable than $^{3}\mathbf{H}_{4}$ for structure **1**. We attribute this result to the fact that the coupled cluster method provides more correct account for the dispersion correction than the M06L functional does. After that, we recalculated the energies of the previously found conformers of glucosyl oxacarbenium cations in Figure 3 at this level to check whether the relative differences between them are reproduced. This functional was also used to calculate the energies of the $^{3}\mathbf{H}_{4}$ conformers. Also, we tried two other DFT functionals, M06 and B3LYP, to compare their results against those of the coupled cluster in order to find out which one

https://doi.org/10.1021/acsomega.4c10086
ACS Omega 2025, 10, 2305−2313

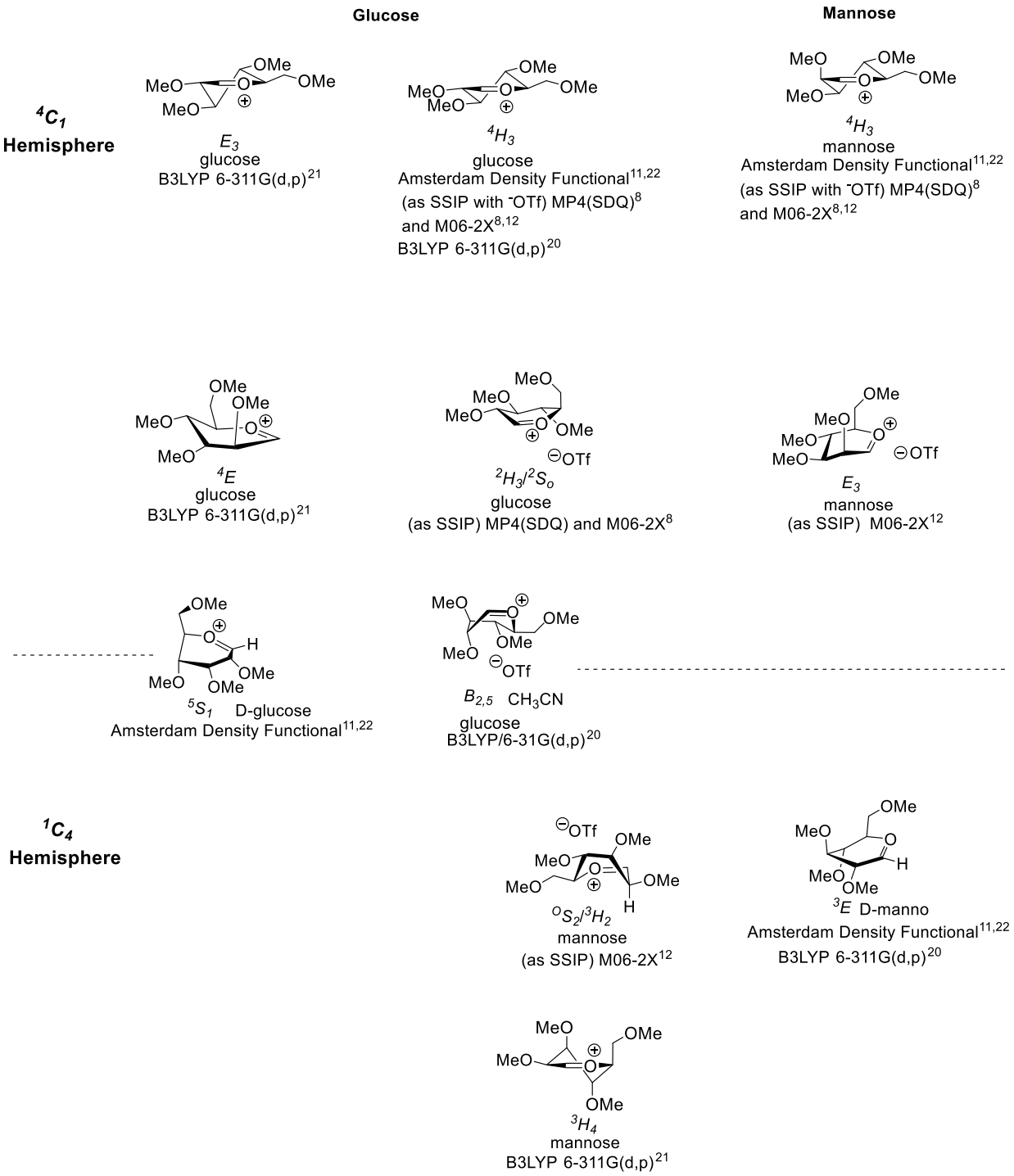

Figure 2. Conformations of permethylated gluco- and manno-oxocarbenium cations and solvent-separated ion pairs (SSIPs) as calculated by quantum mechanical methods.

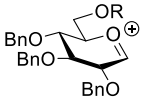

Figure 3. Glycosyl cations studied in this work.

could be recommended for adequate calculations of carbohydrate molecules with all protective groups explicitly included.

Computational Protocols. Calculations were performed with ORCA 5.0.4 software.[25] All of the studied DFT functionals were used with their defaults. The defgrid3 option was switched on throughout the calculations. Grimme's dispersion correction[26] was applied for B3LYP and M06 functionals. The CPCM[27] model with parameters for methylene chloride was applied both for DFT and DLPNO−CCSD(T) calculations.

https://doi.org/10.1021/acsomega.4c10086
ACS Omega 2025, 10, 2305−2313

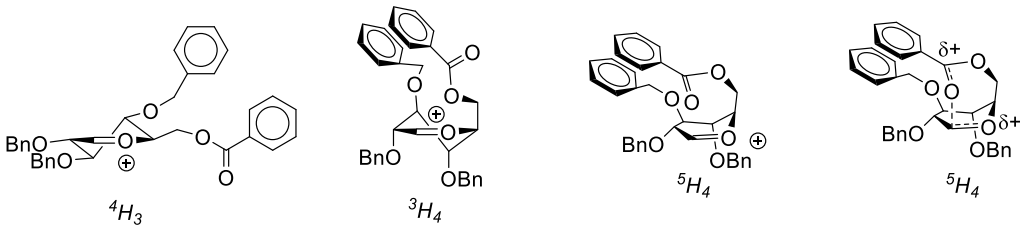

Figure 4. Interactions between phenyl rings in the half-boat conformers of the glucosyl cations.[2122]

Table 1. Comparison of Relative Energies for Conformers of Structures 1−4 Calculated by Different Methods

structure	starting conformer	resulting conformer and relative energy after optimization/relative energy after CCSDT(T) single point, kcal/mol		
		M06L	B3LYP-D3	M06-D3
1	$^4H_3$ *gg*	$^4H_3$: 2.1/0.0	$^4H_3$: 0.3/0.4	$^4H_3$: 3.1/0.3
	$^4H_3$ *gt*	$^4H_3$: 4.4/2.1	$^4H_3$: 2.2/2.5	$^4H_3$: 5.8/2.2
	$^4H_3$ *tg*	$^4H_3$−E_3: 4.1/0.8	$^4H_3$−E_3: 1.6/1.6	$^4H_3$-E_3: 3.8/1.5
	$^3H_4$ *gg*	$^5H_4$: 0.0/0.9	$^5H_4$−$^5S_1$: 0.0/0.0	$^5H_4$−$^5S_1$: 0.0/0.0
	$^3H_4$ *gt*	E_4: 4.1/4.1	E_4: 3.3/3.1	E_4: 6.9/3.2
	$^3H_4$ *tg*	E_4: 4.7/3.9	E_4: 2.5/2.3	E_4: 3.7/2.8
2	$^4H_3$ *gg*	$^4H_3$: 3.0/0.3	$^4H_3$: 1.1/0.6	$^4H_3$: 2.5/1.6
	$^4H_3$ *gt*	$^4H_3$: 3.6/1.2	$^4H_3$−E_3: 2.6/2.1	$^4H_3$: 4.3/2.2
	$^4H_3$ *tg*	$^4H_3$−E_3: 2.0/0.0	$^4H_3$: 1.9/1.8	$^4H_3$: 2.7/3.0
	$^3H_4$ *gg*	$^5H_4$−$^5S_1$: 0.4/1.0	$^5H_4$−$^5S_1$: 0.0/0.0	$^5H_4$−$^5S_1$: 0.0/0.0
	$^3H_4$ *gt*	$^5H_4$−$^5S_1$: 3.6/2.6	$^5H_4$: 4.2/3.1	$^5H_4$: 6.1/3.2
	$^3H_4$ *tg*	$^5H_4$−$^5S_1$: 2.6/1.2	$^5H_4$: 2.6/1.9	$^5H_4$−$^5S_1$: 3.1/1.8
3	$^4H_3$ *gg*	$^4H_3$: 2.0/2.0	$^4H_3$: 2.3/1.4	$^4H_3$−E_3: 2.1/1.9
	$^4H_3$ *gt*	$^4H_3$−E_3: 2.1/2.2	$^4H_3$−E_3: 3.6/2.9	$^4H_3$−E_3: 3.0/2.5
	$^4H_3$ *tg*	$^4H_3$−E_3: 0.0/0.0	$^4H_3$: 0.9/0.7	$^4H_3$−E_3: 0.0/0.0
	$^3H_4$ *gg*	$^5H_4$−E_4: 2.7/4.5	$^5H_4$: 1.3/1.6	$^5H_4$−E_4: 4.6/4.2
	$^3H_4$ *gt*	E_4: 2.5/3.8	E_4: 4.4/3.7	E_4: 4.8/2.6
	$^3H_4$ *tg*	$^5H_4$−E_4: 0.8/1.3	$^5H_4$−E_4: 0.0/0.0	$^5H_4$−E_4: 1.4/0.6
4	$^4H_3$ *gg*	$^4H_3$: 2.5/2.5	$^4H_3$: 2.5/3.0	$^4H_3$: 1.5/1.7
	$^4H_3$ *gt*	$^4H_3$: 4.7/4.4	$^4H_3$: 4.2/4.6	$^4H_3$: 4.7/4.1
	$^4H_3$ *tg*	$^4H_3$−E_3: 1.1/0.0	$^4H_3$: 0.6/0.3	$^4H_3$: 0.1/0.0
	$^3H_4$ *gg*	$^3H_4$−E_4: 0.0/1.1	E_4: 1.0/1.4	E_4: 0.0/0.2
	$^3H_4$ *gt*	E_4: 3.9/5.4	E_4: 5.2/4.9	E_4: 5.9/4.2
	$^3H_4$ *tg*	$^5H_4$−E_4: 1.6/1.2	$^5H_4$−E_4: 0.0/0.0	E_4: 1.7/0.6

Initial values for the torsional parameters were chosen as follows: O5−C5−C6−O6 torsion was set to −60° for *gg* rotamers; +60° for *gt* rotamers and to 180° for *tg* rotamers. Initial torsion values for the O2, O3, and O4 benzyl substituents were set to 0° for Hn-Cn-On-CH_2 and to ±30° for H(CH_2)−C(CH_2)−C−C(ortho) and H(CH_2)−C(CH_2)−C−C′(ortho).

RESULTS AND DISCUSSION

Study of the Rotation around the C5−C6 Bond and of the $^4H_3 \leftrightarrow {}^3H_4$ Equilibrium. The energies of the conformers for structures **1**−**4** were calculated using M06L functional and B3LYP and M06 functionals with Grimme's dispersion correction: third order for B3LYP and zeroth order for M06. B3LYP was also tried without the dispersion correction. However, it failed to converge the optimization even in the case of 2,3,4,6-*O*-benzylated cation **1** in the *trans*−*gauche* conformation. This means that pure B3LYP obviously cannot be applied for the modeling of these complex structures and it was not used further. Additionally, this failure confirms the idea that the correct account for the dispersion interactions is crucial in this case.

The results are presented in Table 1. They include the starting and final ring conformations of the studied structures along with the energies obtained for the resultant geometries at DFT and DLPNO−CCSD(T) levels. Remarkably, when the molecules with the starting $^4H_3$ conformation of the monosaccharide ring were subjected to the geometry optimizations, this conformation was retained in all cases with occasional slight distortions toward the envelope conformation. Contrary to that, all molecules with the starting $^3H_4$ ring underwent significant transformations either to the envelope (E_4) or to the distorted $^5H_4$. Only in the case of *gauche*−*gauche* conformation of structure **4**, the final conformation slightly resembled $^3H_4$. All conformations were determined using the Cremer−Pople[28] calculator created by Shinya Fushinobu, available at http://enzyme13.bt.a.u-tokyo.ac.jp/CP. The numerical descriptors for each structure can be found in the Supporting Information.

Study of the Possible C═O/Cation Interactions and Orientation of the Fluorine-Substituted Phenyl Ring.

https://doi.org/10.1021/acsomega.4c10086
ACS Omega 2025, 10, 2305−2313

While the pentafluorobenzoate group is symmetrical, for 2,4,5-trifluorobenzoate, two different orientations of the phenyl ring are possible (Figure 5) with the spatial proximity between the *orto*-fluorine atom and either carbonyl or ester oxygene.

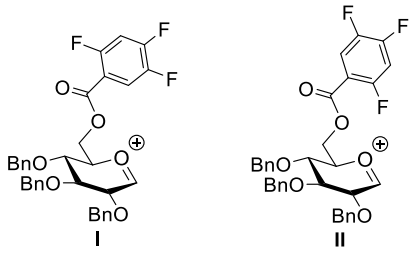

Figure 5. Depictions of the possible rotamers **I** and **II** in cation **3** bearing the 2,4,5-trifluorobenzoyl group at O-6.

Table 2 illustrates how the compared computational methods characterize the energy changes in these conformers. Also, the computed results for the possible anchimeric assistance from the carbonyl oxygen atom to the cationic center at C1 in 6-*O*-acylated structures (Figure 6A) **2**−**4** are given.

Some values in Table 2 are negative, because the energies in each case are calculated relative to the zero-energy conformers from Table 1. In four cases for compounds **3** and **4**, where the starting conformations provided the possibility of the anchimeric assistance, the geometry optimization led to the transformation of the $^{3}\mathbf{H}_{4}$ conformer into $^{1}\mathbf{C}_{4}$ due to the formation of a new C1−O linkage (Figure 6B). It can be seen that, again, the starting $^{4}\mathbf{H}_{3}$ conformations are retained during the geometry optimizations, while the $^{3}\mathbf{H}_{4}$ conformations are transformed into more or less distorted $^{5}\mathbf{H}_{4}$.

It is noteworthy that the results of our calculations seem to contradict to those reported by Martin et al.,[29] who studied experimentally conformations of 2-deoxy- and 2-bromo-

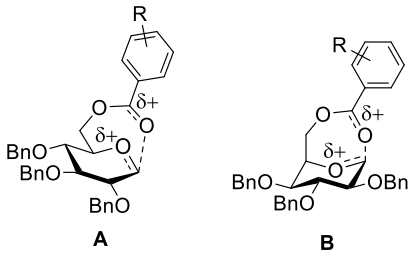

Figure 6. Possible anchimeric assistance from the carbonyl oxygen to the cationic center (**A**) and formation of the $^{1}\mathbf{C}_{4}$ conformer (**B**).

glucosyl oxocarbenium ions stabilized with HF/SbF_5 superacid. They found that these conformations were $^{4}\mathbf{H}_{5}$ and $^{4}\mathbf{E}$, that is, inverted relative to that obtained in this work, $^{5}\mathbf{H}_{4}$ and $\mathbf{E}_{4}$. However, this apparent contradiction is easily explained by a closer examination of the corresponding structure (Figure 7). It is seen that, in our case, ring substituents become axial, making possible planar and orthogonal phenyl ring interactions. Obviously, acetyl groups in work[29] lack such interactions and remain equatorial. This, in our opinion, is another argument for the necessity of the correct account for dispersion interactions. The boat conformer occurring once for cation **2** with the B3LYP-D3 method is also described as possible for oxocarbenium ions.[20,30,31] We believe that this confirms the accuracy of the results of our calculations.

In order to analyze the comparative performance of the three studied DFT functions, the differences in relative electronic energies (from Tables 1 and 2) produced by them and by the DLPNO−CCSD(T) approach for the obtained optimized structures were calculated as $E_{CCSD(T)}-E_{DFT}$. The results are plotted in Figure 8. It can be seen that generally these values for the B3LYP-D3 method are close to zero, while for the other two functionals, more significant deviations are observed. In the case of the M06L functional, these deviations tend to be positive suggesting that the relative conformational

Table 2. Comparison of Relative Energies for Conformers of Structures 2−4 Calculated by Different Methods

structure	starting conformer	resulting conformer and relative energy after optimization/relative energy after CCSDT(T) single point, kcal/mol		
		M06L	B3LYP-D3	M06-D3
2	$^{4}\mathbf{H}_{3}$ *gg*,C=O assistance	$^{4}\mathbf{H}_{3}$−$\mathbf{E}_{3}$: 3.1/0.4	$^{4}\mathbf{H}_{3}$: 1.5/1.1	$^{4}\mathbf{H}_{3}$−$\mathbf{E}_{3}$: 2.6/1.7
	$^{3}\mathbf{H}_{4}$ *gg*,C=O assistance	$^{5}\mathbf{H}_{4}$−$\mathbf{E}_{4}$: 2.5/1.0	$^{2,5}\mathbf{B}$: 2.1/2.1	$^{5}\mathbf{H}_{4}$−$^{5}\mathbf{S}_{1}$: 3.7/3.0
	$^{3}\mathbf{H}_{4}$ *gt*,C=O assistance	$^{5}\mathbf{H}_{4}$−$^{5}\mathbf{S}_{1}$: 2.6/1.2	$^{5}\mathbf{H}_{4}$−$^{5}\mathbf{S}_{1}$: 3.1/1.9	$^{5}\mathbf{H}_{4}$: 5.1/2.0
3	$^{4}\mathbf{H}_{3}$ *gg*, phenyl ring rotamer **II**	$^{4}\mathbf{H}_{3}$: 0.6/0.1	$^{4}\mathbf{H}_{3}$: 1.6/1.4	$^{4}\mathbf{H}_{3}$: 1.0/0.2
	$^{4}\mathbf{H}_{3}$ *gt* phenyl ring rotamer **II**	$^{4}\mathbf{H}_{3}$−$\mathbf{E}_{3}$: 2.1/1.9	$^{4}\mathbf{H}_{3}$−$\mathbf{E}_{3}$: 2.7/2.9	$\mathbf{E}_{3}$: 3.0/1.9
	$^{4}\mathbf{H}_{3}$ *tg*, phenyl ring rotamer **II**	$^{4}\mathbf{H}_{3}$−$\mathbf{E}_{3}$: −0.2/−0.6	$^{4}\mathbf{H}_{3}$: 0.3/−0.1	$^{4}\mathbf{H}_{3}$−$\mathbf{E}_{3}$: 0.1/−1.1
	$^{3}\mathbf{H}_{4}$ *gg*, phenyl ring rotamer **II**	$\mathbf{E}_{4}$: −1.1/−1.3	$\mathbf{E}_{4}$: 0.1/−0.4	$^{5}\mathbf{H}_{4}$−$\mathbf{E}_{4}$: 6.4/4.6
	$^{3}\mathbf{H}_{4}$ *gt*, phenyl ring rotamer **II**	$\mathbf{E}_{4}$: 2.4/3.5	$\mathbf{E}_{4}$: 4.3/3.5	$\mathbf{E}_{4}$: 4.5/2.5
	$^{3}\mathbf{H}_{4}$ *tg*, phenyl ring rotamer **II**	$^{5}\mathbf{H}_{4}$−$\mathbf{E}_{4}$: −1.2/−1.7	$\mathbf{E}_{4}$: −0.3/−0.6	$^{5}\mathbf{H}_{4}$−$\mathbf{E}_{4}$: 1.4/0.6
	$^{4}\mathbf{H}_{3}$ *gg*,C=O assistance	$\mathbf{E}_{3}$: 1.3/1.5	$^{4}\mathbf{H}_{3}$: 0.3/0.7	$^{4}\mathbf{H}_{3}$: 2.4/1.5
	$^{3}\mathbf{H}_{4}$ *gg*,C=O assistance	$\mathbf{E}_{4}$: 2.3/0.7	[a]	[a]
	$^{3}\mathbf{H}_{4}$ *gt*,C=O assistance	$\mathbf{E}_{4}$: 2.5/4.0	$\mathbf{E}_{4}$: 4.3/3.7	$\mathbf{E}_{4}$: 5.2/3.0
	$^{4}\mathbf{H}_{3}$ *gg*, phenyl ring rotamer **II** with C=O assistance	$^{4}\mathbf{H}_{3}$: 0.9/0.9	$^{4}\mathbf{H}_{3}$: 2.7/2.6	$^{4}\mathbf{H}_{3}$: −0.5/0.0
	$^{3}\mathbf{H}_{4}$ *gg*, phenyl ring rotamer **II** with C=O assistance	$^{5}\mathbf{H}_{4}$−$\mathbf{E}_{4}$: −0.1/0.5	[a]	[a]
	$^{3}\mathbf{H}_{4}$ *gt*, phenyl ring rotamer **II** with C=O assistance	$\mathbf{E}_{4}$: 2.4/3.7	$\mathbf{E}_{4}$: 4.1/3.8	$\mathbf{E}_{4}$: 5.0/2.8
4	$^{4}\mathbf{H}_{3}$ *gg*, C=O assistance	$^{4}\mathbf{H}_{3}$: 3.2/2.7	$^{4}\mathbf{H}_{3}$: 3.6/3.6	$\mathbf{E}_{3}$: 3.5/3.4
	$^{3}\mathbf{H}_{4}$ *gg*, C=O assistance	$\mathbf{E}_{4}$−$\mathbf{E}_{1}$: 0.6/1.1	[a]	$\mathbf{E}_{4}$−$\mathbf{E}_{1}$:−0.5/0.7
	$^{3}\mathbf{H}_{4}$ *gt*, C=O assistance	$\mathbf{E}_{4}$: 4.1/5.3	$\mathbf{E}_{4}$: 3.0/2.9	$\mathbf{E}_{4}$: 6.3/4.4

[a]Transformation of the ring into chair conformation occurred during the geometry optimization.

https://doi.org/10.1021/acsomega.4c10086
ACS Omega 2025, 10, 2305−2313

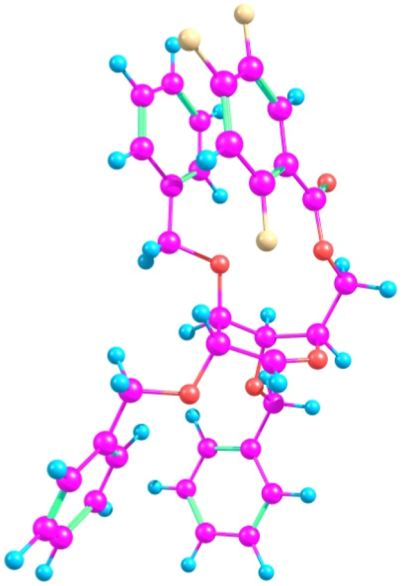

Figure 7. E_4 conformer of cation **3** displaying planar (O6−O3 substituents) and orthogonal (O2−O4 substituents) phenyl interactions.

energies are underestimated by this DFT method. Contrary to that, relative energies resulting from the M06-D3 calculations are usually larger than the corresponding CCSD(T), as is seen from the negative energy differences for this method. As a quantitative characteristic to illustrate the above findings, the averaged absolute differences between the DFT and CCSD(T) energies for each of the three functionals were calculated. It had a value of 1.3 kcal/mol for M06-D3, 0.4 kcal/mol for B3LYP-D3, and 0.8 kcal/mol for M06L. Thus, it can be said that the M06 functional with the additional zeroth-order dispersion correction performs even somewhat worse than the simple M06L with its intrinsic account for the dispersion interactions.

Table 3 demonstrates total SCF energies and correlation corrections (doubles and triples) extracted from DLPNO−CCSD(T) calculations for conformers of cations **1**−**4** obtained via B3LYP-D3 optimization. It can be seen that generally, if a conformer is disfavored by the simple SCF approximation, this can be partly compensated for by applying correlation corrections. Practically, this means that factors that seem disfavoring at first glance (sterical repulsion of the aromatic substituents in our case) may, on the contrary, appear stabilizing when the electronic correlation is properly considered. Thus, we suggest that in cases when the computations are carried out on carbohydrate molecules containing explicit protecting groups, especially with aromatic rings, such as benzyl, benzoate, and derivatives thereof, B3LYP-D3 should be considered as a method of choice for the calculations.

Table 3. Comparison of the Total SCF Energy and Summary Correlation Energies for Different Conformers of Cations 1−4 Preliminary Optimized with B3LYP-D3

structure	B3LYP-D3 optimized conformer	SCF energy from DLPNO−CCSD(T) calculation, a.u.	total correlation energy from DLPNO−CCSD(T) calculation, a.u.
1	$^4H_3$ *gg*	−1682.57581459	−7.035532580
	$^4H_3$ *gt*	−1682.57495548	−7.032980305
	$^4H_3$−E_3 *tg*	−1682.56835185	−7.040923061
	$^5H_4$−$^5S_1$ *gg*	−1682.56497976	−7.046916205
	E_4 *gt*	−1682.57413817	−7.032767542
	E_4 *tg*	−1682.56509127	−7.043064581
2	$^4H_3$ *gg*	−1756.33227971	−7.232575010
	$^4H_3$−E_3 *gt*	−1756.33358279	−7.228969719
	$^4H_3$ *tg*	−1756.32325798	−7.239672496
	$^5H_4$−$^5S_1$ *gg*	−1756.32035462	−7.245517560
	$^5H_4$ *gt*	−1756.33449111	−7.226421427
	$^5H_4$ *tg*	−1756.32539805	−7.237516694
3	$^4H_3$ *gg*	−2052.98178545	−7.961497048
	$^4H_3$−E_3 *gt*	−2052.98165370	−7.960509147
	$^4H_3$ *tg*	−2052.97365685	−7.972457076
	$^5H_4$ *gg*	−2052.97045015	−7.974144190
	E_4 *gt*	−2052.98427851	−7.956942605
	$^5H_4$−E_4 *tg*	−2052.97168083	−7.975488282
4	$^4H_3$ *gg*	−2250.72545017	−8.450682368
	$^4H_3$ *gt*	−2250.72809936	−8.445420200
	$^4H_3$ *tg*	−2250.72080413	−8.459685035
	E_4 *gg*	−2250.71358747	−8.465121923
	E_4 *gt*	−2250.73005399	−8.443096546
	$^5H_4$−E_4 *tg*	−2250.71554169	−8.465364312

After the most accurate DFT method was established and the most stable glycosyl cation conformations were identified for each O-6 substituent, these conformation data were then used to investigate the mechanism behind the α-directing influence of benzoyl and polyfluorinated benzoyl substituents. These protective groups have previously been found useful[24] in

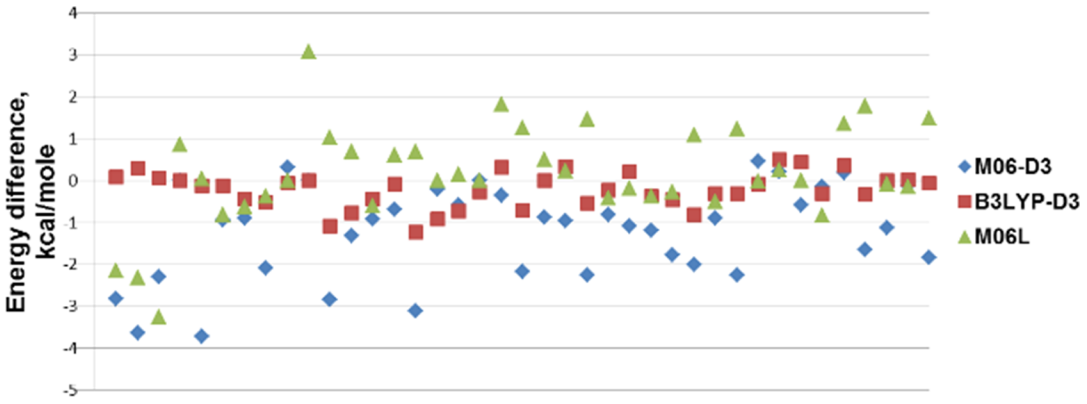

Figure 8. Plot of energy differences for the studied conformers between DLPNO−CCSD(T) and the three DFT functionals employed.

https://doi.org/10.1021/acsomega.4c10086
ACS Omega 2025, 10, 2305−2313

Table 4. Comparison of the Stereochemical Outcomes of Model Glycosylations Using Glucosyl PTFAI Donors with Bn, Bz, TFB, and PFB at O-6, with the Most Favorable Conformation of the Corresponding Glycosyl Cation Formed from These Donors

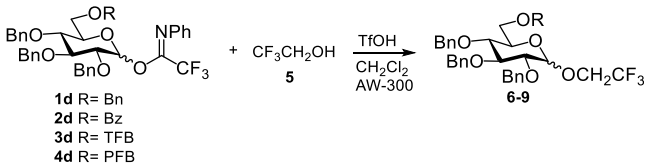

donor (α/β)	R	acceptor	product, α/β (yield)[a]	the most stable conformer (B3LYP-D3, the values of O5−C5−C6−O6 torsion are given in parenthesis)	other low-energy conformers (B3LYP-D3, the values of O5−C5−C6−O6 torsion are given in parenthesis)
1d (1:1.8)	Bn	**5**	**6**α/β, 1.7:1 (86%)[b]	$^5\mathbf{H}_4$−$^5\mathbf{S}_1$ *gg* (−48°): 0.0	$^4\mathbf{H}_3$ *gg* (−71°): 0.3 $^4\mathbf{H}_3$−$\mathbf{E}_3$ *tg* (174°): 1.6
2d (1.3:1)	Bz	**5**	**7**α/β, 3.1:1 (83%)[b]	$^5\mathbf{H}_4$−$^5\mathbf{S}_1$ *gg* (−67°): 0.0	$^4\mathbf{H}_3$ *gg* (−67°): 1.1 $^4\mathbf{H}_3$ *gg* assistance (−82°): 1.5
3d (0:1)	TFB	**5**	**8**α/β, 3.5:1 (95%)[b]	$^1\mathbf{C}_4$ 1,6 assistance (two phenyl ring rotamers, −74°): −3.8, −3.6	$\mathbf{E}_4$ *gg* phenyl ring rotamer II (−51°): −0.3 $^5\mathbf{H}_4$-$\mathbf{E}_4$ *tg* (−172°): 0.0
4d (1.7:1)	PFB	**5**	**9**α/β, 3.4:1 (95%)[b]	$^1\mathbf{C}_4$ 1,6-assistance (−72°): −1.2	$^5\mathbf{H}_4$−$\mathbf{E}_4$ *tg* (−172°): 0.0 $^4\mathbf{H}_3$ *tg* (−175°): 0.6

the preparation of α-glucosides as their presence enhanced α-selectivity, though the underlying mechanism remained incompletely understood. The benzoyl group at the O-6 position is thought to potentially provide remote anchimeric assistance. In contrast, polyfluorinated benzoyl groups, with their carbonyl oxygens of lower nucleophilicity, are not typically considered to be suitable for such assistance. However, the findings from the DLPNO−CCSD(T)/B3LYP-D3 calculations reveal a surprising outcome: polyfluorinated benzoyls do indeed provide remote anchimeric assistance sometimes resulting in the ring inversion to $^1\mathbf{C}_4$ (Table 2). Such inversion only occurs in the case of the fluorine-containing cations. Nevertheless, the benzoyl group still induces α-selectivity, albeit to a weaker extent. Further details on these findings are discussed below.

The most stable glucosyl cation conformations were compared with the stereoselectivity outcomes of model glucosylations involving trifluoroethanol (Table 4). Using the low-nucleophilicity acceptor trifluoroethanol under identical glycosylation conditions (constant temperature, leaving group, reagent concentrations, and promoter), we aimed to establish S_N1-like[32] kinetic conditions. In this context, we propose that the conformation of the oxocarbenium ion serves as the primary determinant of selectivity and a correlation between the lowest-energy conformation and the observed stereoselectivity in glucosylations could be identified.

The introduction of a benzoyl group at O-6 in donor **2d** increases the α/β ratio to 3.1:1 (Table 4, Entry 2) relative to the perbenzylated donor **1d** (Entry 1). This shift in stereoselectivity corresponds to changes in the ratio of the $^5\mathbf{H}_4$ *gg* to $^4\mathbf{H}_3$ *gg* conformations. Specifically, in the perbenzylated donor **1d**, the $^4\mathbf{H}_3$ *gg* and $^5\mathbf{H}_4$ *gg* conformations are energetically equivalent, whereas in the 6-*O*-benzoylated donor **2d**, the $^4\mathbf{H}_3$ *gg* conformation is 1.1 (0.6) kcal/mol higher in energy. Based on this observation, the $^4\mathbf{H}_3$ *gg* conformation can be associated with the formation of the β-product. This conclusion aligns with the general understanding that the $^4\mathbf{H}_3$ conformer is pro-β. With a benzoyl group at O-6, the conformer associated with remote anchimeric assistance ($^4\mathbf{H}_3$ *gg*) was 1.5 kcal/mol higher in energy, indicating that the $^5\mathbf{H}_4$ *gg* conformer plays a significant role in α-product formation. Detailed analysis of the $^5\mathbf{H}_4$ *gg* conformer reveals that the gg orientation of the side chain enhances α-selectivity by effectively shielding the β-side from nucleophilic attack through the spatial positioning of the 6-O fragment.

Attaching a trifluorobenzoyl group to O-6 surprisingly favors two $^1\mathbf{C}_4$ conformers, differing only in the orientation of the nonsymmetric 2,4,5-trifluorophenyl ring in TFB (Figure 5), both representing 1,6-anchimeric assistance (Entry 3). There is a significant energy gap of 3.0−3.5 kcal/mol between these $^1\mathbf{C}_4$ conformers and the nonassisting $\mathbf{E}_4$ *gg* and $^5\mathbf{H}_4$-$\mathbf{E}_4$ *tg* conformers. Consequently, the α/β ratio of 3.5:1 is attributed to remote anchimeric assistance by TFB at O-6.

Remote 1,6-anchimeric assistance is also observed when a PFB group is present at O-6, although the energy difference between the $^1\mathbf{C}_4$ (assistance-related) conformer and the $^4\mathbf{H}_3$ *tg* (pro-α) and $^5\mathbf{H}_4$-$\mathbf{E}_4$ *tg* conformers is smaller, at 0.6 and 1.2 kcal/mol, respectively (Entry 4). This energy difference still supports an α/β ratio of 3.4:1, which can be attributed to remote 1,6-assistance.

The observed similarity in stereoselectivity between TFB- (**3d**) and PFB-protected (**4d**) donors, despite differences in their computationally predicted remote participation, suggests that the α-selectivity in the oxocarbenium ion is influenced by multiple factors. For PFB donor **4d**, where remote participation is weaker, the specific factors driving the α-selectivity remain unclear at this stage. Further investigation is needed to identify these contributors and provide a more complete mechanistic understanding.

From these results, it is evident that, according to DLPNO−CCSD(T) and B3LYP-D3 calculations, anchimeric assistance by acyl substituents at the position of O−6 is somewhat stronger with TFB and PFB than with the more nucleophilic Bz. This discrepancy can be explained by the indirect influence of complex mutual interactions between the aromatic groups of the 2,3,4-tri-*O*-benzyl substituents and the functionalized benzoyl group, which were revealed by DLPNO−CCSD(T) and B3LYP-D3 calculations.

CONCLUSIONS

Three DFT functionals were tried in order to determine which one could be recommended for adequate calculations of carbohydrate molecules with all protective groups explicitly included. This was done by comparing their results against those from single point DLPNO−CCSD(T) calculations, which were used as the standard for electronic energy

https://doi.org/10.1021/acsomega.4c10086
ACS Omega 2025, 10, 2305−2313

estimation. SCF energies and the electronic correlation energies as produced by DLPNO−CCSD(T) suggest that the dispersion correction plays an important role in this case. It obviously occurs because numerous van der Waals interactions between the substituents take place. Thus, the use of the dispersion correction is absolutely necessary. Among the three studied DFT methods, B3LYP with the third-order Grimme's correction was found to provide most reliable results. This finding was confirmed by a good correlation of the results produced by this approach with some model glycosylations. Thus, the suggested method opens perspective toward correct modeling of glycosylation intermediates with explicit protecting groups which is necessary to choose a strategy in oligosaccharide syntheses.

■ ASSOCIATED CONTENT

Supporting Information

The Supporting Information is available free of charge at https://pubs.acs.org/doi/10.1021/acsomega.4c10086.

Cartesian coordinates, absolute DFT energies, Cremer−Popple parameters, and glycosylation procedures (PDF)

■ AUTHOR INFORMATION

Corresponding Authors

Alexey G. Gerbst − *Laboratory of Glycoconjugate Chemistry, N.D. Zelinsky Institute of Organic Chemistry, Russian Academy of Sciences, Moscow 119991, Russia*; Email: alger@ioc.ac.ru

Nikolay E. Nifantiev − *Laboratory of Glycoconjugate Chemistry, N.D. Zelinsky Institute of Organic Chemistry, Russian Academy of Sciences, Moscow 119991, Russia*; orcid.org/0000-0002-0727-4050; Email: nen@ioc.ac.ru

Authors

Bozhena S. Komarova − *Laboratory of Glycoconjugate Chemistry, N.D. Zelinsky Institute of Organic Chemistry, Russian Academy of Sciences, Moscow 119991, Russia*

Artem N. Vlasenko − *Laboratory of Glycoconjugate Chemistry, N.D. Zelinsky Institute of Organic Chemistry, Russian Academy of Sciences, Moscow 119991, Russia*; orcid.org/0000-0002-8820-9954

Complete contact information is available at: https://pubs.acs.org/10.1021/acsomega.4c10086

Author Contributions

The manuscript was written through contributions of all authors. All authors have given approval to the final version of the manuscript.

Funding

This work was supported by the Ministry of Science and Higher Education of the Russian Federation (Agreement no. 075-15-2024-531).

Notes

The authors declare no competing financial interest.

■ ABBREVIATIONS

TS, transition state; GC, glycosyl cation; PFB, pentafluorobenzoate; TFB, 2,3,5-trifluorobenzoate; Bz, benzoate; Bn, benzyl; PTFAI, *N*-phenyltrifluoroacetimidoyl

■ REFERENCES

(1) Ayala, L.; Lucero, C. G.; Romero, J. A. C.; Tabacco, S. A.; Woerpel, K. A. Stereochemistry of Nucleophilic Substitution Reactions Depending upon Substituent: Evidence for Electrostatic Stabilization of Pseudoaxial Conformers of Oxacarbenium Ions by Heteroatom Substituents. *J. Am. Chem. Soc.* **2003**, *125* (50), 15521−15528.

(2) Smith, D. M.; Woerpel, K. A. Electrostatic Interactions in Cations and Their Importance in Biology and Chemistry. *Org. Biomol. Chem.* **2006**, *4* (7), 1195.

(3) Yang, M. T.; Woerpel, K. A. The effect of electrostatic interactions on conformational equilibria of multiply substituted tetrahydropyran oxacarbenium ions. *J. Org. Chem.* **2009**, *74* (2), 545−553.

(4) Remmerswaal, W. A.; Hansen, T.; Hamlin, T. A.; Codée, J. D. C. Origin of stereoselectivity in S_E2' reactions of six-membered ring oxacarbenium ions. *Chem.—Eur. J.* **2023**, *29*, No. e202203490.

(5) Woods, R. J.; Andrews, C. W.; Bowen, J. P. Molecular mechanical investigations of the properties of oxacarbenium ions. 2. Application to glycoside hydrolysis. *J. Am. Chem. Soc.* **1992**, *114* (3), 859−864.

(6) Gerbst, A. G.; Ustuzhanina, N. E.; Grachev, A. A.; Tsvetkov, D. E.; Khatuntseva, E. A.; Nifant'ev, N. E. Effect of the nature of protecting group at O-4 on stereoselectivity of glycosylation by 4-O-substituted 2,3-di-O-benzylfucosyl bromides. *Mendeleev Commun.* **1999**, *9* (3), 114−116.

(7) Miljković, M.; Yeagley, D.; Deslongchamps, P.; Dory, Y. L. Experimental and theoretical evidence of through-space electrostatic stabilization of the incipient oxacarbenium ion by an axially oriented electronegative substituent during glycopyranoside acetolysis. *J. Org. Chem.* **1997**, *62* (22), 7597−7604.

(8) Hosoya, T.; Takano, T.; Kosma, P.; Rosenau, T. Theoretical foundation for the presence of oxacarbenium ions in chemical glycoside synthesis. *J. Org. Chem.* **2014**, *79* (17), 7889−7894.

(9) Hosoya, T.; Kosma, P.; Rosenau, T. Theoretical study on the effects of a 4,6-O-diacetal protecting group on the stability of ion Pairs from d-mannopyranosyl and d-glucopyranosyl triflates. *Carbohydr. Res.* **2015**, *411*, 64−69.

(10) Gerbst, A. G.; Ustuzhanina, N. E.; Grachev, A. A.; Tsvetkov, D. E.; Khatuntseva, E. A.; Whitfield, D. M.; Berces, A.; Nifantiev, N. E. Synthesis, NMR, and conformational studies of fucoidan fragments. III. Effect of benzoyl group at O-3 on stereoselectivity of glycosylation by 3-O- and 3,4-di-O-benzoylated 2-O-benzylfucosyl bromides. *J. Carbohydr. Chem.* **2001**, *20* (9), 821−831.

(11) Whitfield, D. M. DFT studies of the ionization of alpha and beta glycopyranosyl donors. *Carbohydr. Res.* **2007**, *342*, 1726−1740.

(12) Hosoya, T.; Kosma, P.; Rosenau, T. Contact ion pairs and solvent-separated ion pairs from D-mannopyranosyl and D-glucopyranosyl triflates. *Carbohydr. Res.* **2015**, *401*, 127−131.

(13) Huang, M.; Garrett, G. E.; Birlirakis, N.; Bohé, L.; Pratt, D. A.; Crich, D. Dissecting the mechanisms of a class of chemical glycosylation using primary ^{13}C kinetic isotope effects. *Nat. Chem.* **2012**, *4*, 663−667.

(14) Shanthamurthy, C. D.; Gimeno, A.; Ben-Arye, S. L.; Kumar, N. V.; Jain, P.; Padler-Karavani, V.; Jiménez-Barbero, J.; Kikkeri, R. Sulfation code and conformational plasticity of L-iduronic ccid, homo-oligosaccharides mimic the biological functions of heparan sulfate. *ACS Chem. Biol.* **2021**, *16*, 2481−2489.

(15) Komarova, B. S.; Gerbst, A. G.; Finogenova, A. M.; Dmitrenok, A. S.; Tsvetkov, Y. E.; Nifantiev, N. E. 1,3-*syn*-Diaxial repulsion of typical protecting groups used in carbohydrate chemistry in 3-O-substituted derivatives of isopropyl d-idopyranosides. *J. Org. Chem.* **2017**, *82* (17), 8897−8908.

(16) Csonka, G. I.; Kaminsky, J. Accurate conformational energy differences of carbohydrates: A complete basis set extrapolation. *J. Chem. Theory Comput.* **2011**, *7* (4), 988−997.

(17) Marianski, M.; Supady, A.; Ingram, T.; Schneider, M.; Baldauf, C. Assessing the accuracy of across-the-scale methods for predicting

carbohydrate conformational energies for the examples of glucose and α-maltose. *J. Chem. Theory Comput.* **2016**, *12* (12), 6157−6168.
(18) Moon, S.; Chatterjee, S.; Seeberger, P. H.; Gilmore, K. Predicting glycosylation stereoselectivity using machine learning. *Chem. Sci.* **2021**, *12*, 2931−2939.
(19) Guo, A.; Xu, Y.; Jia, Z.; Loh, T.-P.; Liu, X.-W. Unraveling chemical glycosylation: DFT insights into factors imparting stereoselectivity. *Green Synth. Catal.* **2024**.
(20) Satoh, H.; Hansen, H. S.; Manabe, S.; van Gunsteren, W. F.; Hünenberger, P. H. Theoretical Investigation of Solvent Effects on Glycosylation Reactions: Stereoselectivity Controlled by Preferential Conformations of the Intermediate Oxacarbenium-Counterion Complex. *J. Chem. Theory Comput.* **2010**, *6*, 1783−1797.
(21) Hansen, T.; Lebedel, L.; Remmerswaal, W. A.; van der Vorm, S.; Wander, D. P. A.; Somers, M.; Overkleeft, H. S.; Filippov, D. V.; Désiré, J.; Mingot, A.; Bleriot, Y.; van der Marel, G. A.; Thibaudeau, S.; Codée, J. D. C. Defining the SN1 Side of Glycosylation Reactions: Stereoselectivity of Glycopyranosyl Cations. *ACS Cent. Sci.* **2019**, *5*, 781−788.
(22) Nukada, T.; Bérces, A.; Wang, L. J.; Zgierski, M. Z.; Whitfield, D. M. The two-conformer hypothesis: 2,3,4,6-tetra-O-methyl-mannopyranosyl and -glucopyranosyl oxacarbenium ions. *Carbohydr. Res.* **2005**, *340*, 841−852.
(23) Komarova, B. S.; Wong, S. S. W.; Orekhova, M. V.; Tsvetkov, Y. E.; Krylov, V. B.; Beauvais, A.; Bouchara, J.-P.; Kearney, J. F.; Aimanianda, V.; Latgé, J.-P.; Nifantiev, N. E. Chemical Synthesis and Application of Biotinylated Oligo-α-(1→3)-D-Glucosides To Study the Antibody and Cytokine Response against the Cell Wall α-(1→3)-D-Glucan of *Aspergillus fumigatus*. *J. Org. Chem.* **2018**, *83*, 12965−12976.
(24) Komarova, B. S.; Novikova, N. S.; Gerbst, A. G.; Sinitsyna, O. A.; Rubtsova, E. A.; Kondratyeva, E. G.; Sinitsyn, A. P.; Nifantiev, N. E. Combination of 3-O-levulinoyl and 6-O-trifluorobenzoyl groups ensures α-selectivity in glucosylations: Synthesis of the oligosaccharides related to *Aspergillus fumigatus* α-(1→3)-D-glucan. *J. Org. Chem.* **2023**, *88* (17), 12542−12564.
(25) Neese, F. The ORCA program system. *Wiley Interdiscip. Rev.:Comput. Mol. Sci.* **2012**, *2*, 73−78.
(26) Grimme, S.; Antony, J.; Ehrlich, S.; Krieg, H. A consistent and accurate *ab initio* parametrization of density functional dispersion correction (DFT-D) for the 94 elements H-Pu. *J. Chem. Phys.* **2010**, *132*, 154104.
(27) Barone, V.; Cossi, M. Quantum calculation of molecular energies and energy gradients in solution by a conductor solvent model. *J. Phys. Chem. A* **1998**, *102*, 1995−2001.
(28) Cremer, D.; Pople, J. A. A General definition of ring puckering coordinates. *J. Am. Chem. Soc.* **1975**, *97*, 1354−1358.
(29) Martin, A.; Arda, A.; Désiré, J.; Martin-Mingot, A.; Probst, N.; Sinaÿ, P.; Jiménez-Barbero, J.; Thibaudeau, S.; Blériot, Y. Catching elusive glycosyl cations in a condensed phase with HF/SbF5 superacid. *Nat. Chem.* **2016**, *8*, 186−191.
(30) Merino, P.; Delso, I.; Pereira, S.; Orta, S.; Pedrón, M.; Tejero, T. Computational evidence of glycosyl cations. *Org. Biomol. Chem.* **2021**, *19*, 2350−2365.
(31) Franconetti, A.; Ardá, A.; Asensio, J. L.; Blériot, Y.; Thibaudeau, S.; Jiménez-Barbero, J. Glycosyl Oxocarbenium Ions: Structure, Conformation, Reactivity,and Interactions. *Acc. Chem. Res.* **2021**, *54*, 2552−2564.
(32) Van Der Vorm, S.; Hansen, T.; Overkleeft, H. S.; Van Der Marel, G. A.; Codée, J. D. C. The influence of acceptor nucleophilicity on the glycosylation reaction mechanism. *Chem. Sci.* **2017**, *8* (3), 1867−1875.

https://doi.org/10.1021/acsomega.4c10086
ACS Omega 2025, 10, 2305−2313